Quantal and Thermal Dampings of Giant Dipole Resonances in ^{90}Zr, ^{120}Sn, and ^{208}Pb

Nguyen Dinh Dang and Akito Arima
Cyclotron Laboratory, RIKEN, Wako, Saitama 351-01, Japan
(Received 3 October 1997)

The damping of the giant dipole resonance (GDR) is studied in ^{90}Zr, ^{120}Sn, and ^{208}Pb as a function of temperature T. The results show that the coupling of GDR to the pp and hh states is responsible for the increase of the GDR width with increasing T up to 3 MeV and its saturation at higher T. The quantal width, caused by the coupling to ph excitations, decreases slowly with increasing T. An overall agreement is found between the theoretical evaluations and the recent experimental data in heavy-ion fusion reactions and inelastic α scattering. At very high T a behavior similar to the transition from zero to ordinary sounds is observed. [S0031-9007(98)06119-5]

PACS numbers: 24.30.Cz, 21.10.Pc, 24.10.Pa, 24.60.–k

The giant dipole resonance (GDR), built on compound nuclear states, has been studied intensively during the last 15 years [1]. The measurements show that the energy of the GDR is rather stable with varying temperature. Its width increases rapidly with increasing excitation energy E^* (or temperature T) up to around 130 MeV in Sn isotopes [2–4]. At higher E^* the width increases slowly and even saturates [3,5–7]. The ground-state GDR (g.s. GDR) acquires an escape width $\Gamma^\uparrow$ via a γ or particle emission and a spreading (or quantal) width $\Gamma^\downarrow$ by coupling to more complicated configurations. The extension of the microscopic approaches in [8,9] to $T \neq 0$ shows only a little change of $\Gamma^\downarrow$ [10,11]. Shape fluctuations are taken into account to describe the increase in the width at $T \neq 0$. The new experimental methods involving compound nuclear reactions [12] and inelastic α scattering [13] allow separating the effects due to thermal fluctuations and due to angular momentum in the study of hot GDR. The recent calculations in [14], including the thermal shape fluctuations and the evaporation width [15], agree nicely with the data of [13] for the GDR width in ^{120}Sn and ^{208}Pb at 1 MeV $< T \leq 3$ MeV. The effects of angular momentum J are important only at rather high $J \geq 35\hbar$ at $T \simeq 1.5-1.8$ MeV and only in a lighter nucleus ^{106}Sn [16]. Recently, we have demonstrated in [17] that the coupling of the GDR excitation to the pp and hh configurations, which appear at $T \neq 0$, leads to the thermal damping of the GDR. In this Letter, elaborating further this concept, we will perform a systematic study of the width of the hot GDR in ^{90}Zr, ^{120}Sn, and ^{208}Pb in a large range of temperature up to at least $T \sim 6$ MeV.

The coupling of collective oscillations (phonons) to the field of ph, pp, and hh pairs can be studied using the model Hamiltonian:

$$H = \sum_s E_s a_s^\dagger a_s + \sum_q \omega_q Q_q^\dagger Q_q + \sum_{ss'q} F_{ss'}^{(q)} a_s^\dagger a_{s'} (Q_q^\dagger + Q_q) . \tag{1}$$

The first term on the right-hand side (RHS) of Eq. (1) describes the field of independent single particles $a_s^\dagger$ and a_s. The second term stands for the phonon field $\{Q_q^\dagger, Q_q\}$. The last term describes the coupling between the first two fields. $E_s = \epsilon_s - \epsilon_F$, where ϵ_s is the single-particle energy and ϵ_F—the Fermi surface energy. We will simply refer to the energy E_s as single-particle energy. The phonon energy is denoted as ω_q.

We introduce the double-time Green's functions [18], which describe (a) *the propagation of a free particle (or hole):* $G_{s;s'}(t - t') = \langle\langle a_s(t); a_{s'}^\dagger(t')\rangle\rangle$; (b) *the propagation of a free phonon:* $G_{q;q'}(t - t') = \langle\langle Q_q(t); Q_{q'}^\dagger(t')\rangle\rangle$; (c) *the particle-phonon coupling in the single-particle field:* $\Gamma^-_{sq;s'}(t - t') = \langle\langle a_s(t) Q_q(t); a_{s'}^\dagger(t')\rangle\rangle$, and $\Gamma^+_{sq;s'}(t - t') = \langle\langle a_s(t) Q_q^\dagger(t); a_{s'}^\dagger(t')\rangle\rangle$; (d) *the transition between a nucleon pair and a phonon:* $\mathcal{G}^-_{ss';q}(t - t') = \langle\langle a_s^\dagger(t) a_{s'}(t); Q_q^\dagger(t')\rangle\rangle$. A hierarchy of coupled equations for Green's functions is obtained, following the standard procedure. We close this hierarchy to the functions in (a)–(d) using the decoupling scheme in [18]. Making the Fourier transformation to the energy plane E and eliminating functions $\Gamma^-(E)$, $\Gamma^+(E)$, and $\mathcal{G}(E)$ by expressing them in terms of $G_{s;s'}(E)$ and $G_{q;q'}(E)$, we obtain a set of two equations for $G_{s;s'}(E)$ and $G_{q;q'}(E)$, which describe the p (h) and phonon propagations, respectively. For the propagation of a single p (or h) state $s = s'$ and a single phonon state $q = q'$ these equations become

$$G_s(E) = \frac{1}{2\pi}[E - E_s - M_s(E)]^{-1},$$
$$G_q(E) = \frac{1}{2\pi}[E - \omega_q - P_q(E)]^{-1}, \tag{2}$$

where the mass $M_s(E)$ and the polarization $P_q(E)$ operators are

$$M_s(E) = \sum_{q's'} F_{ss'}^{(q')} F_{s's}^{(q')} \left(\frac{v_{q'} + 1 - n_{s'}}{E - E_{s'} - \omega_{q'}} + \frac{n_{s'} + v_{q'}}{E - E_{s'} + \omega_{q'}} \right), \qquad P_q(E) = \sum_{ss'} F_{ss'}^{(q)} F_{s's}^{(q)} \frac{n_s - n_{s'}}{E - E_{s'} + E_s} . \tag{3}$$

0031-9007/98/80(19)/4145(4)$15.00

Closing the hierarchy to the functions (a)–(d) restricts the couplings in $M_s(E)$ to at most $2p1h$ configurations if the one-phonon operator generates the collective ph excitation. The effects of coupling to $2p2h$ configurations can be included by extending the hierarchy to higher-order Green's functions of "$1p1h \oplus$ phonon" type (Figs. 3 and 4 of [10]) or two-phonon type (Fig. 1 of [11]), etc. The numerical calculations in [10,11,19] have shown that the effects of these graphs on $\Gamma^{\downarrow}$ depend weakly on T. In fact $\Gamma^{\downarrow}$ in ^{90}Zr and ^{208}Pb have become even smaller at $T = 3$ MeV in [10]. Therefore, in the present Letter, in order to avoid the complicated procedure of taking these graphs into account microscopically, we consider this effect to be independent of T and include them in the parameters of the model defined at $T = 0$. The dampings $\gamma_s(\omega)$ of the single-particle and $\gamma_q(\omega)$ of the phonon states are derived as the imaginary parts of the analytical continuation in the complex energy plane $\eta = \omega \pm i\epsilon$ of the mass $M_s(e)$ and polarization operators $P_q(E)$, respectively:

$$\gamma_s(\omega) = \pi \sum_{q's'} F_{ss'}^{(q')} F_{s's}^{(q')} [(v_{q'} + 1 - n_{s'})\delta(\omega - E_{s'} - \omega_{q'}) + (n_{s'} + v_{q'})\delta(\omega - E_{s'} + \omega_{q'})], \tag{4}$$

$$\gamma_q(\omega) = \pi \sum_{ss'} F_{ss'}^{(q)} F_{s's}^{(q)} (n_s - n_{s'})\delta(\omega - E_{s'} + E_s). \tag{5}$$

The single-particle occupation number n_s (for phonon v_q) in Eqs. (3)–(5) has the form of a Fermi (Bose) distribution folded with a Lorentzian with a width $2\gamma_s(\omega)\,[2\gamma_q(\omega)]$ and centered at $\tilde{E}_s = E_s + M_s(\tilde{E}_s)\,[\tilde{\omega}_q = \omega_q + P_q(\tilde{\omega}_q)]$. If γ_s is small, n_s can be well approximated by an exact Fermi distribution function with energy $\tilde{E}_s$. For v_q this is not valid because γ_q is large. If the GDR is described by a strongly collective vibration, centered at energy $\omega_q = E_{\rm GDR}(T)$, where $E_{\rm GDR}(T)$ is the pole of $G_q(\omega)$ in Eq. (2), the value $\Gamma_{\rm GDR} = 2\gamma_q[E_{\rm GDR}(T)]$ is its full width at half maximum (FWHM). At $T = 0$, n_s is equal to 1 for a hole state ($E_h < 0$) and 0 for a particle one ($E_p > 0$). Therefore, $\Gamma_{\rm GDR}$ in Eq. (5) has a non zero value only in the sum over ph configurations (the quantal damping), where $n_h - n_p = 1$. As temperature increases, the quantal damping, denoted as Γ_Q, decreases as the difference $n_h - n_p$ decreases from 1 at $T = 0$ to 0 at $T = \infty$. At the same time there appear the pp and hh configurations because the difference $n_s - n_{s'} \neq 0$ also for $(s, s') = (p, p')$ or (h, h') at $T \neq 0$. The coupling to pp and hh configurations leads to the thermal damping Γ_T [17], which increases first with increasing T. However, because of the factor $n_s - n_{s'}$, $\Gamma_{\rm GDR}$ will decrease as $O(T^{-1})$ at large T. Therefore it must reach some plateau within a certain region of temperature. This is a natural explanation for the width saturation within our model. The coupling to pp and hh configurations is a microscopic way of taking into account thermal shape fluctuations. Indeed, a pp or hh pair operator $B_{ss'} = a_s^{\dagger} a_{s'}$ can be expanded as a sum of tensor products of two ph pair operators [20]. If one ph pair operator B_{ph} has the angular momentum and parity of the GDR $J^{\pi} = 1^-$, the other ph pair can have the angular momentum and parity of 2^+, etc., conserving the total angular momentum and parity. Hence, the quadrupole shape fluctuations and higher multipolarities are taken into account. The single-particle damping $\gamma_s(\omega)$ increases at high temperatures as $O(T/\omega)$ according to Eq. (4). At high T one obtains $\gamma_s(\omega_1) < \gamma_s(\omega_2)$ for $\omega_1 > \omega_2$.

We assume for simplicity that the g.s. GDR is generated by a structureless phonon with energy ω_q close to the energy $E_{\rm GDR}(T = 0)$. The single-particle energies are obtained within the Woods-Saxon potentials at $T = 0$ for ^{90}Zr, ^{120}Sn, and ^{208}Pb, whose parameters have been defined in [21]. The matrix elements of the coupling to ph, pp, hh configurations are parameterized as $F_{ph}^{(q)} = F_1$ for $(s, s') = (p, h)$ and $F_{pp}^{(q)} = F_{hh}^{(q)} = F_2$ for $(s, s') = (p, p')$ or (h, h'). The phonon energy ω_q and F_1 are chosen so that the empirical quantal width Γ_Q and energy $E_{\rm GDR}(T = 0)$ [22] are reproduced. F_2 is chosen so that the $E_{\rm GDR}(T)$ remains rather stable with varying temperature. They are kept unchanged at $T \neq 0$. This ensures that all thermal effects are caused by the coupling between the GDR and the single-particle field, but not by changing parameters. We also checked that the GDR sum rule was conserved as temperature was varied. The δ functions on the RHS of Eqs. (4) and (5) is replaced with a Lorentzian with a smearing parameter ϵ. It smooths out narrow peaks and therefore allows calculations on a coarse energy mesh. To avoid spurious results, ϵ has to be chosen sufficiently small. Our results are found to be rather stable in the interval 0.2 MeV $\leq \epsilon \leq$ 1.0 MeV. Those, obtained with $\epsilon = 0.5$ MeV, are discussed below.

The averaged single-particle damping widths $\Gamma_{\rm s.p.}$ reaches a value of 1.4 MeV in ^{90}Zr, 1.6 MeV in ^{120}Sn, and 0.9 MeV in ^{208}Pb at $T = 5$ MeV in the energy region below the GDR. In the region above the GDR energy, $\Gamma_{\rm s.p.} < 0.6$ MeV and rather stable with varying T, in agreement with the behavior $\sim O(T/\omega)$ of $\gamma_s(\omega)$ at high T discussed above. The damping widths of the GDR in ^{120}Sn and ^{208}Pb are displayed as a function of T in Fig. 1 in comparison with the inelastic α scattering data [13]. The quantal width Γ_Q (dashed curve) is obtained via coupling to only ph states. The thermal width Γ_T (dotted curve) comes from the coupling to pp and hh configurations at $T \neq 0$. The total width $\Gamma_{\rm GDR}$ (solid-with-diamond curve) is calculated via coupling to all ph, pp, and hh configurations, including the effect of single-particle damping. It is seen that the quantal effects become weaker in hot GDR as Γ_Q is slowly getting smaller with increasing T. A decrease of the spreading width has also been reported in [10] in ^{90}Zr and ^{208}Pb

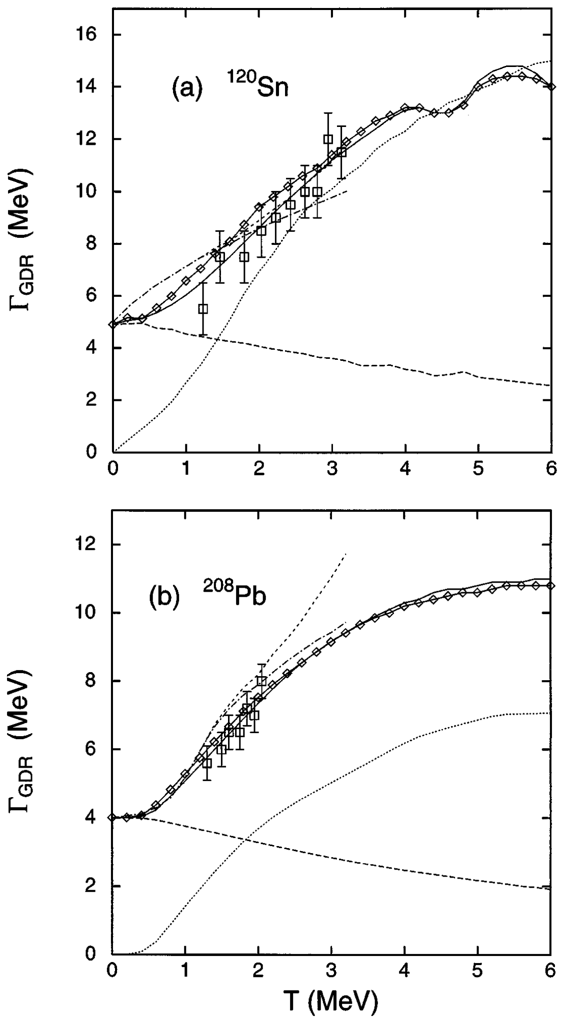

FIG. 1. Width of GDR as a function of temperature for ^{120}Sn (a) and ^{208}Pb (b). Experimental data of [13] are shown by open squares. The dashed curve denotes the quantal width Γ_Q; the dotted curve stands for thermal width Γ_T; the solid curve with diamonds represents the total width $\Gamma_{\rm GDR}$ (see text). The solid curve is $\Gamma_{\rm GDR}$, calculated without the effect of single-particle damping. The dash-dotted and short-dashed curves represent the widths obtained within the adiabatic model [14] without and with the inclusion of the evaporation width, respectively.

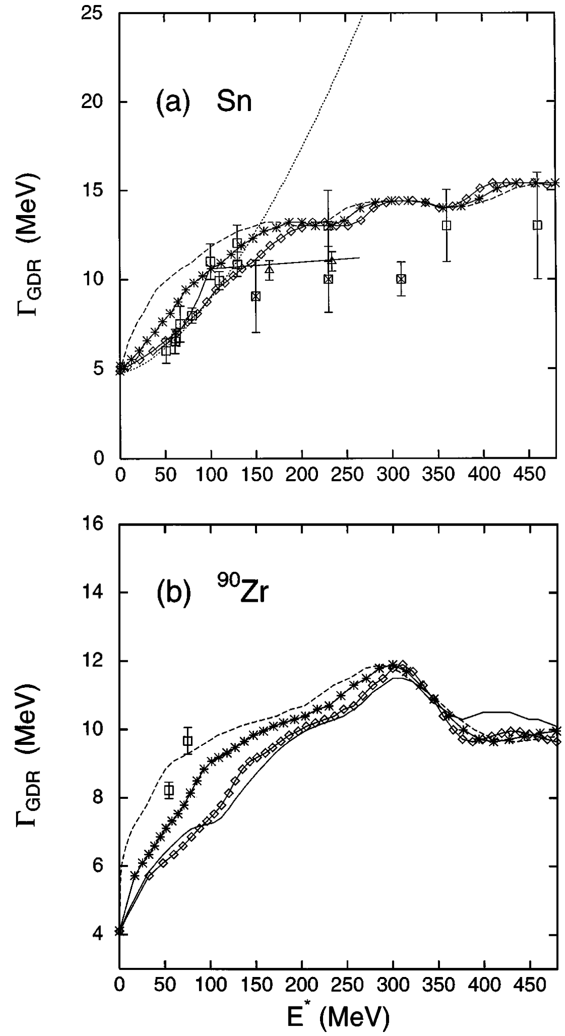

FIG. 2. Width of GDR in Sn (a) and ^{90}Zr (b) as a function of excitation energy. Experimental FWHM from [2,3] (a) and [4] (b) are represented by open squares, while triangles, and crossed-open squares in (a) stand for the data from [5] and [6], respectively. The solid curve with diamonds represents the width $\Gamma_{\rm GDR}$ in our model, plotted as a function of $E^*_{\rm m.f.}$. The dashed curve is the same width, but plotted as a function of $E^*_{\rm F.g.}$. The solid curve with stars is the same width, plotted as a function of $\overline{E}^*$ (See text). The solid curve in (b) is the width $\Gamma_{\rm GDR}$ calculated without the effect of single-particle damping and plotted against $E^*_{\rm m.f.}$. In (a) the widths, obtained in [24] and [25], are shown by the solid and dotted curves, respectively.

at $T = 3$ MeV, including the "$1p1h \oplus$ phonon" graphs. The thermal damping width Γ_T, on the contrary, becomes rapidly larger as T increases. As a result, the total width increases sharply as T rises up to 3 MeV and slowly at higher temperatures. It reaches a saturation (around 14 MeV in ^{120}Sn and 11 MeV in ^{208}Pb) at $T = 4$–6 MeV. These results show that the GDR width at high T is driven mostly by the thermal width Γ_T. Our results agree well with the experimental data. This agreement is also better than the one given in [14]. The effect of the single-particle damping is rather small up to very high temperature (compare the solid curve with diamonds to the solid curves in Fig. 1).

Shown in Fig. 2 is the same width $\Gamma_{\rm GDR}$ in our model for ^{120}Sn and ^{90}Zr, but plotted as a function of E^* in comparison with the FWHM of the GDR from the heavy-ion fusion data in tin isotopes [2,3,7] and in ^{90}Zr [4], and from deeply inelastic reactions [5]. The excitation energy E^* is evaluated in two ways: (i) $E^*_{\rm m.f.} = \epsilon(T) - \epsilon(0)$, where $\epsilon(T)$ is the total energy of the system in the thermal mean field, where the temperature T enters as a parameter after averaging over the grand canonical ensemble [23]; and (ii) $E^*_{\rm F.g.} = AT^2/12$ from the Fermi-gas model. An overall agreement between our results and the data is seen in the whole region of E^*, including $250 \leq E^* \leq 450$ MeV [3,5,6]. The predictions of [24] (solid curve) and [25] (dotted curve) are also shown. They are similar to ours at $E^* \leq 150$ MeV. In this region there is a discrepancy between the dependences of $\Gamma_{\rm GDR}$ on $E^*_{\rm m.f.}$ (solid curve with diamonds) [23] and on $E^*_{\rm F.g.}$ (dashed curve). Collective modes, especially the quadrupole one, also enhance the level density [23] and push $E^*_{\rm m.f.}$ closer to $E^*_{\rm F.g.}$. Therefore the same width is plotted in Fig. 2 versus the value $\overline{E}^* = (E^*_{\rm m.f.} + E^*_{\rm F.g.})/2$ for comparison. The correspondence between T, defined in the thermal mean-field and the effective T, extracted experimentally, still requires further investigation. Hence, these three dependences may serve as a reference guideline.

Shown in Fig. 3 is the same width $\Gamma_{\rm GDR}$ as a function of $E^*_{\rm F.g.}$ up to $E^*_{\rm F.g.} = 900$ MeV. The width saturation is clearly seen in all three nuclei. The widths $\Gamma_< = \Gamma_{\rm GDR}(T = 0) + bT^2$ with $b = 1\ {\rm MeV}^{-1}$ for $\Gamma_{\rm GDR} \ll E_{\rm GDR}$ (zero-sound region) and $\Gamma_> = \Gamma_{\rm GDR}(T = 0) + c(E_{\rm GDR}/T)^2$ with $c = 1$ MeV for $\Gamma_{\rm GDR} \gg E_{\rm GDR}$ (ordinary-sound region) from the Landau theory of Fermi liquids [26] are also plotted with a phase transition point at $T \simeq 4.1$, 3.9, and 3.7 MeV for systems with $A = 90$, 120, and 208, respectively. The behavior of the GDR width in finite nuclei exhibits a quite similar feature to the transition from zero to ordinary sounds in a Fermi liquid. The phase transition is strongly smeared out in hot nuclei. The transition from zero to ordinary sounds in excited nuclear matter has been also discussed in [27] as a possible mechanism of the disappearance of GDR at high T. Other effects, such as the temperature dependence of the single-particle energies, the evaporation with, etc., left out in this study, should show up in this region and contribute in reordering the absolute values of the widths according to the mass number.

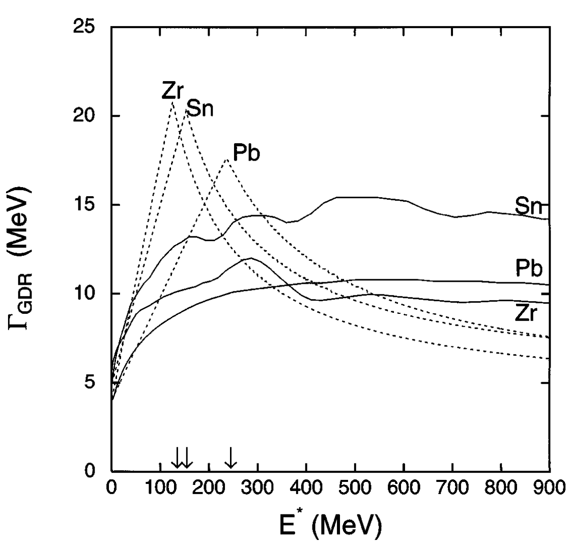

FIG. 3. Width $\Gamma_{\rm GDR}$ as a function of Fermi-gas excitation energy $E^*_{\rm F.g.}$. The solid curves represent $\Gamma_{\rm GDR}$ in ^{90}Zr, ^{120}Sn, and ^{208}Pb. The dotted curves denote the corresponding widths from the Landau theory of Fermi liquids [26]. The arrow shows the energy of the phase-transition point, which is 126, 154, and 237 MeV for $A = 90$, 120, and 208, respectively.

In summary, we have presented a systematic study of the width of GDR in ^{90}Zr, ^{120}Sn, and ^{208}Pb as a function of temperature. An overall agreement between our results and the experimental data is found in a large region $0 \leq T \leq 6$ MeV. We conclude that the coupling of the GDR to the pp and hh, responsible for the thermal width Γ_T, indeed plays a decisive role in the increase of the total width at low E^* and in its saturation at high E^*. The quantal width Γ_Q, caused by the coupling of the GDR to only ph configurations, decreases slowly with increasing T. The effect of single-particle damping is rather small up to high excitation energies. The similarity, observed in this work, between the saturation of the GDR width in finite nuclei and the phase transition from zero to ordinary sounds in a Fermi liquid deserves further studies.

[1] K. Snover, Annu. Rev. Nucl. Part. Sci. **36**, 545 (1986); J. J. Caardhøje, Ann. Rev. Nucl. Part. Sci. **42**, 483 (1992).
[2] J. J. Gaardhøje *et al.*, Phys. Rev. Lett. **53**, 148 (1984); **56**, 1783 (1986); D. R. Chakrabarty *et al.*, Phys. Rev. C **36**, 1886 (1987); A. Bracco *et al.*, Phys. Rev. Lett. **62**, 2080 (1989); D. Perroutsakou *et al.*, Nucl. Phys. **A600**, 131 (1996).
[3] J. J. Gaardhøje *et al.*, Phys. Rev. Lett. **59**, 1409 (1987).
[4] J. H. Gundlach *et al.*, Phys. Rev. Lett. **65**, 2523 (1990).
[5] G. Enders *et al.*, Phys. Rev. Lett. **69**, 249 (1992).
[6] H. J. Hofmann *et al.*, Nucl. Phys. **A571**, 301 (1994).
[7] P. Piatelli *et al.*, Nucl. Phys. **A599**, 63c (1996).
[8] V. G. Soloviev, *Theory of Atomic Nuclei–Quasiparticles and Phonons* (Energoatomizdat, Moscow, 1989).
[9] G. F. Bertsch, P. F. Bortignon, and R. A. Broglia, Rev. Mod. Phys. **55**, 287 (1983).
[10] P. F. Bortignon *et al.*, Nucl. Phys. **A460**, 149 (1986).
[11] N. Dinh Dang, Nucl. Phys. **A504**, 143 (1989).
[12] A. Bracco *et al.*, Phys. Rev. Lett. **74**, 3748 (1995).
[13] E. Ramakrishnan *et al.*, Phys. Rev. Lett. **76**, 2025 (1996).
[14] W. E. Ormand, P. F. Bortignon, and R. A. Broglia, Phys. Rev. Lett. **77**, 607 (1996); W. E. Ormand *et al.*, Nucl. Phys. **A614**, 217 (1997).
[15] Ph. Chomaz, Phys. Lett. B **347**, 1 (1995).
[16] M. Matiuzzi *et al.*, Nucl. Phys. **A612**, 262 (1997).
[17] N. Dinh Dang and F. Sakata, Phys. Rev. C **55**, 2872 (1997).
[18] D. N. Zubarev, Sov. Phys. Usp. **3**, 320 (1960).
[19] P. Donati *et al.*, Phys. Lett. B **383**, 15 (1996).
[20] F. Catara, N. Dinh Dang, and M. Sambataro, Nucl. Phys. **A579**, 1 (1994).
[21] V. A. Chepurnov, Sov. J. Nucl. Phys. **6**, 955 (1967); K. Takeuchi and P. A. Moldauer, Phys. Lett. B **28**, 384 (1969).
[22] B. L. Berman and S. C. Fultz, Rev. Mod. Phys. **47**, 713 (1975).
[23] N. Dinh Dang, A. Phys. A **335**, 253 (1989).
[24] R. A. Broglia, P. F. Bortignon, and A. Bracco, Prog. Part. Nucl. Phys. **28**, 517 (1992).
[25] A. Bonasera *et al.*, Nucl. Phys. **A569**, 215c (1994).
[26] L. D. Landau, Sov. Phys. JETP **5**, 101 (1957).
[27] V. Baran *et al.*, Nucl. Phys. **A599**, 29c (1996).